FEBS 18035 FEBS Letters 401 (1997) 43–48

Aggregation of PDGF-β receptors in human skin fibroblasts: characterization by image correlation spectroscopy (ICS)

Paul W. Wiseman[a], Pia Höddelius[b], Nils O. Petersen[a,*], Karl-Eric Magnusson[c]

[a] *Department of Chemistry, the University of Western Ontario, London, Ontario N6A 5B7, Canada*
[b] *Department of Cell Biology, Faculty of Health Sciences, Linköping University, S-581 85 Linköping, Sweden*
[c] *Department of Medical Microbiology, Faculty of Health Sciences, Linköping University, S-581 85 Linköping, Sweden*

Received 22 April 1996; revised version received 28 November 1996

Abstract Receptor aggregation is believed to be an important, early step when growth factors such as PDGF stimulate proliferation and differentiation of cell populations. To investigate receptor aggregation, we utilized a novel biophysical technique, image correlation spectroscopy, to study the distribution and aggregation state of PDGF-β receptors on the surface of human dermal fibroblasts under various experimental conditions. It was found that the cell surface receptors were pre-clustered at 4°C and receptor aggregation increased for samples measured at 37°C. Treatment with PDGF-BB had no measurable effect on the receptor aggregation state. The results also indicate that additions of 10% serum or an inhibitor of tyrosine kinase activity, may disperse the receptors. The results of this study are consistent with organization of PDGF-β receptors in pre-existing membrane domains.

Key words: Aggregation; PDGF receptor; PDGF; Correlation spectroscopy; Membrane domain

1. Introduction

Platelet-derived growth factor (PDGF) is a major mitogen in serum for cultured mesenchymal, smooth muscle and glial cells. It consists of two, disulfide-linked polypeptide chains, denoted A and B [1], which share 60% homology in their amino acid sequences [2–5]. Three dimeric forms of PDGF exist, viz. PDGF-AA, -AB and -BB, with different functional activities. Two distinct, but structurally related PDGF receptors have been characterized, i.e. the α-receptor and β-receptor [6–9]. The α-receptor binds all three forms of PDGF, whereas the β-receptor binds primarily PDGF-BB, and with lower affinity PDGF-AB. The mechanism by which PDGF exerts its growth factor promoting activity is not fully understood. A number of metabolic changes have been documented to occur rapidly following addition of PDGF. They include receptor autophosphorylation on tyrosine residues, hydrolysis of plasma membrane phospholipids, increase in intracellular free [Ca^{2+}], activation of protein kinase C (PKC) and of Na^+/H^+ exchange, alterations in the structure and organization of cytoskeletal proteins, and changes in gene expression [10–12].

Intra- and intermolecular models of ligand-dependent growth factor kinase activation have been proposed and are widely discussed [13–15]. The combination of biophysical and biochemical experiments have provided important understanding of the mechanism(s) behind the action of growth factor receptors and associated cell signals [5,13].

To elucidate basal mobility characteristics of the PDGF receptor in the fibroblast membrane, and to investigate the effects of serum and PDGF stimulation, experiments were conducted [16,17] utilizing the previously described technique of fluorescence recovery after photobleaching (FRAP) [18–20]. Using this method, it is possible to measure the rate of lateral diffusion and estimate the fraction of mobile PDGF receptors in human fibroblasts. We have recently employed a new technique, image correlation spectroscopy (ICS) [21], a further development of scanning-fluorescence correlation spectroscopy [22], to characterize the distribution and state of aggregation of membrane receptors, specifically PDGF-β receptors. The present report describes ICS analysis of PDGF-β receptor clustering at 4 and 37°C, and as affected by PDGF-BB, serum and tyrosine kinase inhibition treatments.

A major reason for studying membrane receptor dynamics and surface distributions is their relevance to biological function of receptors at a molecular level. Evidence has accumulated that the molecular organization and lateral distribution of receptors in cell membranes are important for their function [13,23,24]. It is possible that most receptors are neither randomly nor homogeneously distributed, but rather partly aggregated. Moreover, the distribution of receptors on the cell surface often changes as a consequence of receptor-ligand interactions [25]. Obvious questions to be answered are therefore: Are the receptors uniformly or randomly distributed? Do they reside within domains on the cell surface prior to the binding of ligand? If clusters exist, can their surface density and size be determined? What are their lateral mobilities? Answers to these and related questions will influence the way we understand the dependence of cellular response on changes in receptor mobility, receptor-receptor interactions and receptor-ligand interactions.

2. Materials and methods

2.1. Cell culture

Human foreskin fibroblasts (AG1523; Human Genetic Cell Repository, Camden, NJ) were maintained at 37°C in a humidified incubator at 5% CO_2 (type CO_2-AutoZero; Hereus, Hanau, Germany) in Eagle's minimum essential medium (Gibco Ltd., Paisley, UK) supplemented with 10% fetal calf serum, penicillin (50 IU/ml) and streptomycin (50 μg/ml). The cells were sub-cultured on 12 mm glass coverslips in Petri dishes, both in the same type of medium to yield 'normal' cells, and in MCDB 105 medium (Gibco, Ltd.) with 1 mg/ml serum albumin added after 3 days to yield 'starved' cells, i.e. cells from serum-free growth conditions. In all cases the cells were used on day 5 after plating.

*Corresponding author.

Abbreviations: CLSM, confocal laser scanning microscopy; EGF, epidermal growth factor; FRAP, fluorescence recovery after photobleaching; ICS, image correlation spectroscopy; PDGF-BB, platelet-derived growth factor (BB); PDGFR-β, platelet-derived growth factor receptor-beta; PKC, protein kinase C

PII S0014-5793(96)01429-9

2.2. Cell labeling

Monoclonal antibodies directed specifically toward the PDGF-β receptor (PDGFR-B2) [26] were either kindly provided by Dr. C.-H. Heldin, Ludwig Institute for Cancer Research, Uppsala, Sweden, or purchased from Sigma Chemical Co. (no. P-7679, St. Louis, MO). The antibody has been shown to bind to the extracellular part of the PDGF-β receptor. It does not inhibit ^{125}I-PDGF binding to the receptor, but does precipitate the receptor in suspension. On cells the antibody induces receptor patches. An FITC-labeled goat-anti-mouse IgG antibody, specific for the Fc portion of the mouse monoclonal antibody (no. F-5387, Sigma Chemical Co., St. Louis, MO) was used as a secondary antibody. The cells were first pre-incubated at 37°C for 10 min, and then incubated successively with the primary and secondary antibodies for 30 min on ice. The primary antibodies were used at a 1:10 dilution from stock concentration and the secondary antibodies at a 1:5 dilution for labeling purposes to ensure saturating labeling conditions. Before addition of the secondary antibody, the cells were washed in Krebs-Ringer glucose-containing phosphate buffer with 10 mM glucose and 1 mM Ca^{2+} and Mg^{2+}, pH 7.3, KRG. PDGF-BB was a kind gift from Dr. C.-H. Heldin. Some samples were treated with 20 ng/ml PDGF-BB following immunolabeling of the cells. In separate experiments the growth factor was demonstrated to be active at concentrations as low as 1 ng/ml on AG1523 cells (data not shown). The erbstatin analog was a product of Calbiochem-Novabiochem Corp. (San Diego, CA). To achieve inhibition of tyrosine phosphorylation, some cells were preincubated with 5 μg/ml erbstatin analog, for 10 min at 37°C. The medium was then removed and the cells put on ice before the labeling procedure. Erbstatin analog was present during the measurements.

2.3. Image correlation spectroscopy (ICS)

The theoretical and experimental basis for ICS has recently been presented [21]. Briefly, the surface distribution of fluorescently stained PDGF-β receptors was measured via confocal laser scanning microscopy (CLSM) [27] using a Phoibos 1000 microscope (Molecular Dynamics, Sunnyvale, CA). ICS analysis was carried out on confocal images which were obtained at the highest possible magnification using a 100×, 1.3 N.A. objective, yielding a pixel resolution of 0.1 μm in both the *x*- and *y*-directions (Fig. 1B). These 'high magnification' images were collected to ensure that none of the areas outside of the cell (as visible in Fig. 1A) were sampled. The high zoom confocal images were utilized for autocorrelation analysis, and were transferred electronically from the Silicon Graphics Iris Indigo workstation of the Phoibos 1000 microscope in Linköping to a VAX 6430 mainframe computer at the Information Technology Services of the University of Western Ontario (London, ON, Canada). ICS programs were implemented on the VAX mainframe to calculate a two-dimensional spatial autocorrelation function from each confocal image. The zero lag (central) amplitude of the resulting discrete autocorrelation function (the $g(0,0)$ value) was determined via a non-linear least-squares fitting procedure (Fig. 1C). As has been described previously, the $g(0,0)$ value is in fact the average number of independent fluorescent entities within an area defined by the focused laser beam on the cell surface [21]. The average surface density of labeled receptors (the cluster density) is then directly calculated via a simple conversion factor from the $g(0,0)$ value and the focal spot area of the laser beam (the beam area is calculable from the laser beam radius which is also obtained as a parameter from the fitting to the autocorrelation data) [21].

3. Results

3.1. Effect of temperature and PDGF-BB on PDGFR-β aggregation

To study the effect of PDGF and temperature independently, live cells were labeled at 4°C, then transferred to a temperature-controlled microscope stage (4 ± 0.2°C), where PDGF-BB was added after 5 min. The spatial distribution of the labeled receptors was then recorded by scanning a confocal image at a fixed optical plane on a specific area of the membrane of an individual cell. A time series of confocal images was collected from an individual sample at 5-min intervals for a total of 35 min with a different cell being imaged for each sample time. Multiple time series were collected on identically prepared samples. The mean surface density of labeled receptors in each image (the receptor cluster density) was calculated using the ICS technique as described above. The average number of receptor clusters varied between 8 and 12 per μm^2 (Fig. 2A). Each time point is the average of 11–19 different samples obtained on 4–5 occasions. No effect of PDGF-BB addition was seen. The frequency distribution of cluster densities for these samples is shown in Fig. 3A. As images are sampled from individual cells, the frequency distribution reflects a sampling of the inherent variation in cluster density in the cell population. A large variation in cluster density among individual cells is detected.

In the second set of experiments, the stage temperature was increased to 37(±0.2°C), and PDGF-BB was again added after 5 min. In this case, the cluster density was a factor 3–4 lower, i.e. around 3–4 clusters per μm^2 (Fig. 2B). No statistically significant effect of PDGF-BB was observed, although the cluster density decreased gradually with time after addition of PDGF-BB. The frequency distribution of the cluster densities for the intact cells at 37°C is presented in Fig. 3C and is much narrower than that for the cells at 4°C. This reflects a more homogeneous receptor aggregation state for the cell population at the higher temperature.

3.2. Receptor distribution on paraformaldehyde-fixed cells

Cells were sequentially incubated with primary and secondary antibodies for 30 min (15 min primary and 15 min secondary IgG) or 120 min (60 min primary and 60 min secondary IgG) on ice. The cells were subsequently fixed in 4% paraformaldehyde. The cluster densities in fixed cells were similar to the values obtained for live cells at 4°C, i.e. around 12 clusters per μm^2 (Fig. 2A). The frequency distribution of cluster densities is presented for the 30 min incubation (Fig. 3B) and is analogous to that for the intact cells at 4°C (Fig. 3A). The differences in symmetry between these two distributions may be attributed to the fact that in Fig. 3A, the data reflect a range of incubation times over 35 min while the paraformaldehyde data (Fig. 3B) is effectively a 'snapshot' of the receptor distribution at a single time. However, the similarity in the spread of the two 4°C distributions is evident.

3.3. Effect of serum and tyrosine kinase inhibition on receptor distribution

The experiments involving treatment of the cells with serum or erbstatin analog were performed as time series experiments in a manner similar to those previously described. However, a limited number of time series were run for these experiments. To facilitate comparisons, the data were averaged across the time series as there was little temporal variation between time points at 4 and 37°C (Fig. 2A,B). This allowed for grouped comparisons between the data from different experiments (Fig. 4), but entailed the loss of any temporal trends contained in the time series. Nevertheless, the smaller number of series run for the last two experiments precluded resolution of any temporal trends from the data anyway.

On a limited number of samples, we employed ICS to characterize the 4°C distribution of receptors after adding serum at time zero. Interestingly, the cluster density increased following addition of the serum to the samples (Fig. 4).

A number of samples were pre-treated with an analog of

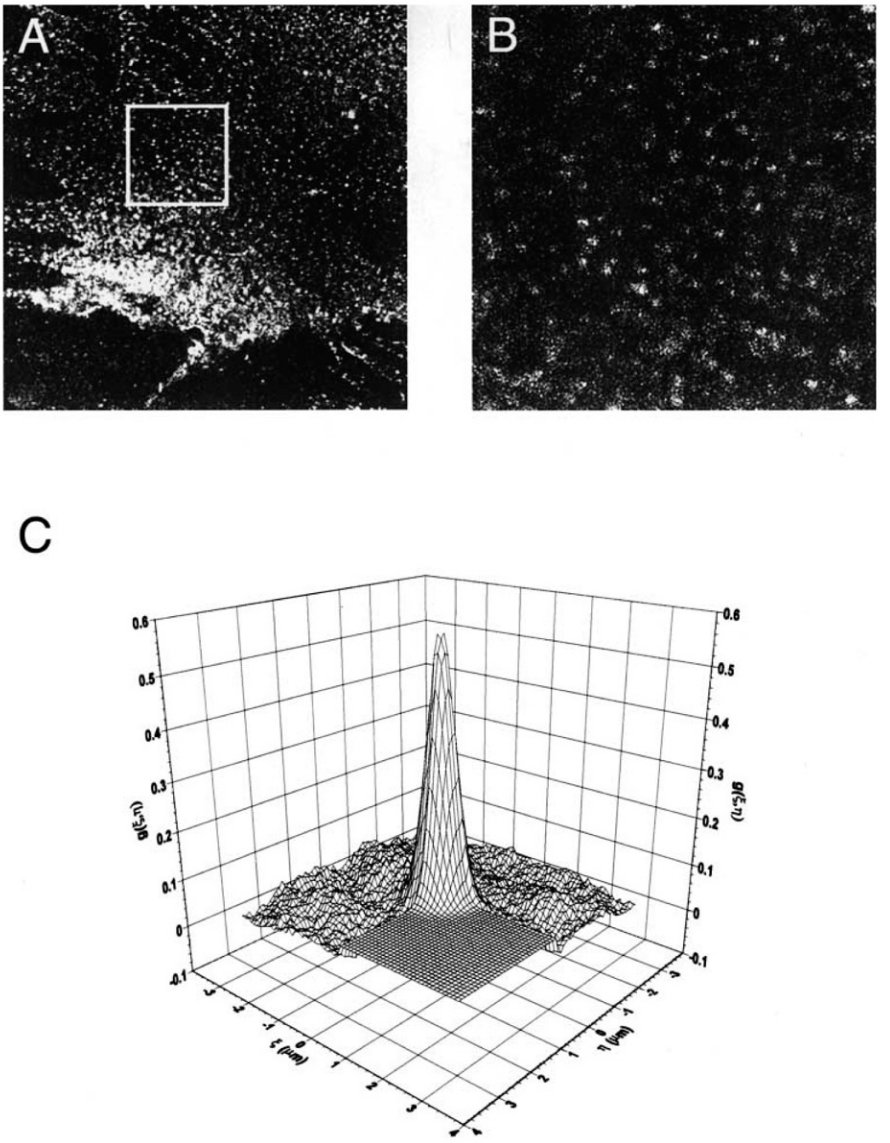

Fig. 1. (A) Overview (low magnification) confocal image of an AG1523 fibroblast showing labeled PDGF-β receptors. The image has dimensions of 102.4 μm×102.4 μm. (B) High magnification 'zoom' image of labeled PDGF-β receptors sampled from the area enclosed by the white square overlay on the cell depicted in (A). The image has dimensions of 25.6 μm×25.6 μm. (C) Autocorrelation function with function of best fit in near quadrant. This discrete autocorrelation function was calculated from the confocal image shown in (B). The $g(0,0)$ value of this function is inversely proportional to the number of spatially independent labeled receptors per laser beam focal area.

the tyrosine kinase inhibitor erbstatin (5 μg/ml) at 37°C before immunolabeling and confocal imaging at 4°C, and an apparent dispersion of receptors was observed via ICS measurements (higher cluster densities; Fig. 4). However, when PDGF-BB was added together with the erbstatin analog at time 0, the dispersion effect of erbstatin analog was attenuated (Fig. 4).

4. Discussion

Dimerization and aggregation of PDGF receptors have been postulated to play a crucial role in ligand-induced receptor signaling [5,14,15,28]. It is, however, extremely difficult to evaluate the degree of dimerization and aggregation by direct visual inspection of the distribution of fluorescently tagged receptors in the membrane. To address questions of receptor aggregation state we recently presented image correlation spectroscopy [21], which was initially applied to the distribution of PDGF receptors in fixed, dermal fibroblasts. That approach has now been extended to the study of PDGF-β receptors in living fibroblasts at 4 and 37°C, and under the influence of PDGF-BB, serum and erbstatin analog treatment.

With ICS we can compare the number of receptor clusters per unit membrane area on different cell population samples. However, absolute quantification of receptor cluster density requires experimental control of background fluorescence arising from autofluorescence and non-specific binding of fluorophore (Wiseman et al., in preparation). Such controls are relatively easy to implement with fixed cell preparations, but the nature of the time series measurements on living cells precluded inclusion of these controls in the experiments. Therefore, the results presented in this report have not been corrected for background fluorescence contributions and are biased slightly toward higher cluster densities. Although not

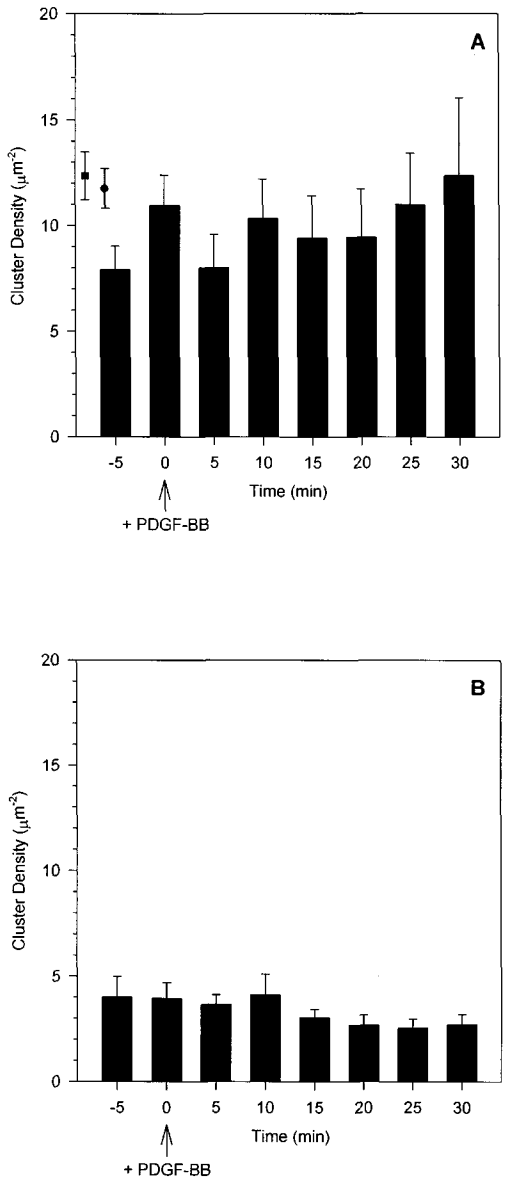

Fig. 2. Cluster density (per μm^2) of PDGF-β receptors at 4 and 37°C, as assessed with image correlation spectroscopy (ICS): (A) average cluster densities ± S.E.M. at 4°C. The separate data points represent the average cluster densities of the samples labeled for 120 min (square) and 30 min (circle) at 4°C with subsequent fixation using 4% paraformaldehyde. (B) Average cluster densities ± S.E.M. at 37°C. Platelet-derived growth factor (PDGF-BB) was added at time zero for both the 4 and 37°C samples.

accurate in the absolute sense, the cluster densities may be used comparatively to demonstrate changes in the underlying state of receptor aggregation. Valid comparisons may be made between samples measured under identical collection conditions, and this criterion was adhered to in the experiments presented in this report.

The results depicted in Fig. 2A,B show that the receptor cluster density is lower by a factor of 3–4 at 37°C as compared to 4°C. This reflects an increasingly aggregated receptor distribution at the higher temperature (fewer clusters containing larger numbers of receptor subunits). Also, addition of PDGF-BB at time zero caused no detectable change in the state of receptor aggregation. Interpretation of the aggregation at 37°C as an antibody induced effect is consistent with the results. Primary and secondary immunolabeling was carried out with whole antibodies which are able to physically crosslink receptors due to the bivalent nature of the IgG molecule. Previous work has demonstrated that the PDGFR-B2 IgG induces clustering of PDGF-β receptors [21,26]. The change in the receptor aggregation state observed here is probably due to rapid crosslinking of the receptors by primary and secondary IgG label at 37°C. At 4°C the diffusive mobility of the receptors is greatly reduced, so addition of the IgG label at this temperature cannot lead to antibody induced crosslinking of receptors. Consequently, measurements on ice effectively sample the underlying receptor distribution while antibody induced clustering is only observed when the samples are warmed to 37°C (Figs. 2A,B and 4).

The absence of an effect of PDGF-BB on the receptor aggregation state may be due to the fact that the antibody label induces a maximum cross-linking of the receptor subunits and the added growth factor binds to the previously clustered receptors. Determination of the effect of PDGF-BB by itself would require immunolabeling with monovalent Fab fragments to remove any confounding effect of IgG induced clus-

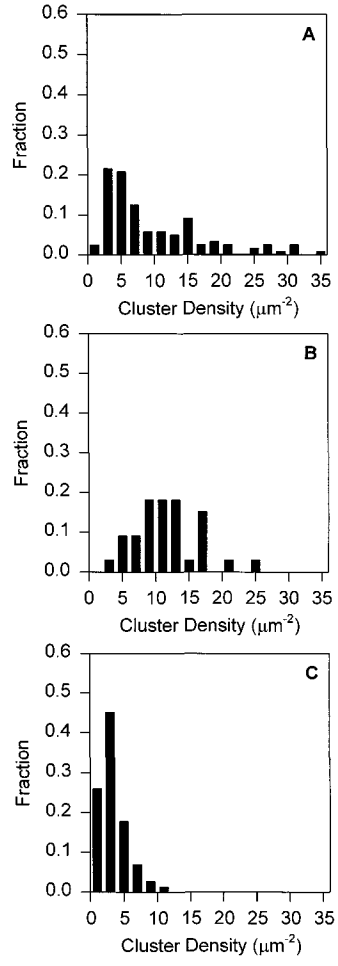

Fig. 3. Frequency histograms of PDGF-β receptor cluster densities for sample data presented in Fig. 2. (A) Histogram of PDGF-β receptor cluster densities for intact cells at 4°C. (B) Frequency histogram of cluster densities of PDGF-β receptors at 4°C as assessed with ICS on cells fixed with 4% paraformaldehyde after 30 min of immunolabeling on ice. (C) Cluster density histogram for intact cell samples at 37°C.

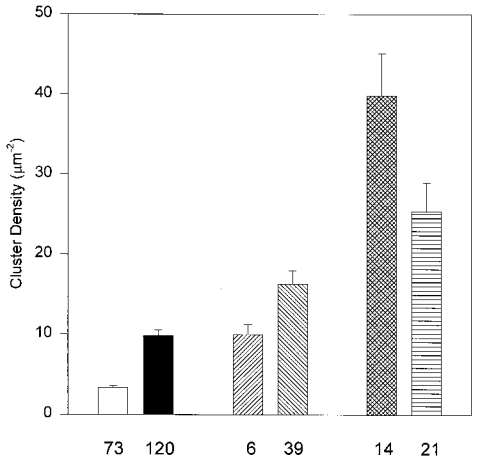

Fig. 4. Summary of mean cluster density data (per μm^2) averaged across the time series for labeled PDGF-β receptors under various treatment conditions. The white bar is the time-independent average cluster density for the 37°C samples from times −5 to 30 min. The black bar represents the analogous mean value for the 4°C samples from times −5 to 30 min. The hatched bar (slanted up from left to right) is the average cluster density of the −5 min samples from the 10% serum experiment (samples at 4°C prior to addition of serum). The other hatched bar (slanted down from left to right) is the average cluster density calculated from the remaining images in the time series for the 10% serum experiment: times 0 to 30 min (all samples at 4°C after addition of the serum). The cross-hatched bar shows the average cluster density calculated from the time series data from time 0 to 30 min for the samples treated with erbstatin analog at time 0. The bar with the horizontal line fill depicts the average cluster density calculated from the time series data from time 0 to 30 min for the samples treated with erbstatin analog and PDGF-BB at time 0. Note that all samples in the final two experiments had been pre-incubated with erbstatin analog at 37°C before immunolabeling and confocal imaging were conducted at 4°C. The error bars represent the S.E.M. while the numbers below the column bars indicate the number of images included in the calculation of the average (i.e. the number of independent cells sampled).

tering. However, such an experiment requires ultra-sensitive fluorescence detection with the confocal microscope as there is a significant reduction in the amount of bound fluorophore when Fab labeling is employed. Photon counting detection may be beneficial for faintly labeled samples as would be the case for Fab labeling, but this collection mode was not available on the instrument used in these experiments.

Comparison of the results obtained for intact cells at 4°C and paraformaldehyde fixed specimens at the same temperature showed essentially equivalent cluster densities (Figs. 2A and 3A,B) This result is significant as it demonstrates that paraformaldehyde fixation has no artefactual effect on the underlying receptor aggregation state and establishes the equivalence of measurements on intact and fixed samples. As measurements on fixed specimens are easily implemented, more data may be accumulated from fixed preparations allowing more reliable assessments of changes in cell population parameters.

The variation in cluster density among individual cells is much greater at 4°C than at 37°C (Fig. 3A,C). This reflects a heterogeneous distribution of receptors in clusters of various size across the surface of different cells. The distribution in cluster density at the lower temperature reflects a direct sampling of the underlying range within the cell population. At 37°C, the antibody label clusters the more dispersed receptor subunits which leads to a concomitant narrowing of the distribution of detected cluster densities (Fig. 3C).

Comparison of the grouped data between different experiments (the averages across time series depicted in Fig. 4) allows assessment of global changes in the aggregation state of PDGF-β receptors in the cell population following various treatments. Addition of serum to the cells seemed to cause a slight dispersion of the receptor population (Fig. 4). Although the results were calculated from a small number of samples, they are consistent with earlier work on the effect of serum on PDGF-β receptor mobilities [16,17]. As has been noted, addition of serum increased the diffusion coefficient and mobile fraction of PDGF-β receptors as detected in these FRAP studies. If addition of serum does indeed lead to dispersion of receptors from aggregates, an increase in mobility would be detected if the receptor subunits diffuse more rapidly than the larger aggregates. This is an intuitively reasonable assumption and demonstrates that the ICS measurements are consistent with the earlier FRAP experiments. These preliminary results suggest that some component in the serum may disperse receptor aggregates, but more data is needed to confirm this.

The erbstatin analog, which is a specific inhibitor of tyrosine kinase activity, also appears to further disfavor receptor clustering (Fig. 4). It appears as though pre-treatment of the cells with the erbstatin analog at 37°C leads to a significant dispersion of the receptors, and this underlying dispersed distribution is effectively sampled by subsequent addition of the immunolabel at 4°C (Fig. 4). Interestingly, addition of PDGF-BB in addition to erbstatin analog at time 0 induces greater clustering of the receptors than observed in the presence of the kinase inhibitor alone (Fig. 4). This contrasts with the previous experiments where addition of PDGF-BB had no discernible effect. A possible explanation is that the erbstatin analog completely disperses the receptors from clusters so that a uniform distribution of monomeric subunits occurs at the surface. In this case, a dimerization event caused by addition of PDGF-BB would be manifest in an ICS measurement. The data show a 40% increase in aggregation for samples treated with PDGF-BB in addition to the tyrosine kinase inhibitor (Fig. 4). In the other experiments involving addition of the growth factor, the receptors were detected in a pre-clustered state. Dimerization of receptor subunits by PDGF-BB within existing clusters would not be detectable via ICS measurement as such an event would not change the global aggregation state across the surface of the cell. The pre-clustering of receptor subunits may explain why no effect of PDGF-BB was detected.

If the erbstatin analog leads to a complete dispersion of the receptor subunits, then the receptors are pre-clustered in aggregates containing on average four subunits at 4°C (tetramers). Based on this assumption, we would estimate that the antibody crosslinked aggregates contain on average 12 receptor subunits (Fig. 4).

As these results suggest, PDGF-BB and erbstatin analog have opposite effects on the distribution of receptors within aggregates, and it would be challenging to investigate further the combined effects of these compounds.

It is surprising that the addition of both serum and erbstatin analog/PDGF-BB has a measurable effect on the state of receptor aggregation at 4°C, whereas the antibody label has no crosslinking effect at this temperature. The reason for this

paradoxical effect is unknown and warrants further investigation.

To summarize, the present study demonstrates that PDGF-β receptors are pre-clustered without ligand addition at 4°C, but the extent of clustering varies greatly between cells. This evidence of small clusters of PDGF-β receptors on the cell surface raises questions as to the physical nature and biological function of these clusters. It was recently reported that epidermal growth factor (EGF) receptors were sequestered in small domains on the surface of mouse keratinocyte cells [29]. The detection of pre-clustered PDGF-β receptors on intact cells at 4°C provides empirical evidence for membrane domain structure on human dermal fibroblasts. At 37°C the receptors are further clustered either naturally or by crosslinking effects of the antibody label. Preliminary results show that certain agents (serum and erbstatin analog) may act to disperse receptor subunits from aggregates. Further studies will be focused on addressing whether further dimerization due to PDGF within these clusters occurs and can be detected with ICS, and whether the clusters may form reaction centers for different ligand-induced cellular responses.

Acknowledgements: Kajsa Holmgren is gratefully thanked for experienced advice on the confocal microscope. This research was supported by grants from the Swedish Society for Medical Research, the Lions Foundation, the Swedish Medical Association, the Magn. Bergvall Foundation, the Swedish Medical Research Council (Project Nos. 4486 and 6251), the Swedish Research Council for Engineering Sciences, the Swedish Telecom Co. Research Foundation, and the Natural Sciences and Engineering Research Council, Canada. P.W.W. was a Postgraduate Fellow of the Natural Sciences and Engineering Research Council, Canada.

References

[1] Johnsson, A., Heldin, C.-H., Westermark, B. and Wasteson, Å. (1982) Biochem. Biophys. Res. Commun. 104, 66–74.
[2] Heldin, C.-H., Westermark, B. and Wasteson, Å. (1981) Biochem. J. 193, 907–913.
[3] Ross, R., Raines, E.W. and Bowen-Pope, D.F. (1986) Cell 46, 155–169.
[4] Heldin, C.-H. and Westermark, B. (1989) Br. Med. Bull. 45, 453–463.
[5] Raines, E.W., Bowen-Pope, D.F. and Ross, R. (1990) in: Peptide Growth Factors and Their Receptors (Sporn, M.B. and Roberts, A.B. eds.) Handbook of Experimental Pharmacology, vol. 95, part I, pp. 173–262, Springer, Heidelberg.
[6] Bishayee, S., Ross, A.H., Womer, R. and Scher, C.D. (1986) Proc. Natl. Acad. Sci. USA 83, 6756–6760.
[7] Claesson-Welsh, L., Eriksson, A., Morén, A., Severinsson, L., Ek, B., Östman, A., Betsholtz, C. and Heldin, C.-H. (1988) Mol. Cell Biol. 8, 3476–3486.
[8] Claesson-Welsh, L., Eriksson, A., Westermark, B. and Heldin, C.-H. (1989) Proc. Natl. Acad. Sci. USA. 86, 4917–4921.
[9] Claesson-Welsh, L., Hammacher, A., Westermark, B., Heldin, C.-H. and Nistér, M. (1989) J. Biol. Chem. 264, 1742–1747.
[10] Berridge, M.S. and Irvine, R.F. (1984) Nature 312, 315–321.
[11] Coughlin, S.R., Lee, W.M., Williams, P.W., Giels, G.W. and Williams, L.T. (1985) Cell 43, 243–251.
[12] Herman, B. and Pledger, W.J. (1985) J. Cell Biol. 100, 1031–1040.
[13] Schlessinger, J.Y. (1988) Trends Biochem. Sci. 13, 443–447.
[14] Lemmon, M.A. and Schlessinger, J. (1994) Trends Biochem. Sci. 19, 459–463.
[15] Heldin, C.-H. (1995) Cell 80, 213–223.
[16] Ljungquist, P., Wasteson, Å. and Magnusson, K.-E. (1989) Biosci. Rep. 9, 63–73.
[17] Ljungquist-Höddelius, P., Lirvall, M., Wasteson, Å. and Magnusson, K.-E. (1991) Biosci. Rep. 11, 43–52.
[18] Jacobson, K., Derzko, Z., Wu, E.S., Hou, Y. and Poste, G. (1976) J. Supramol. Struct. 5, 556–565.
[19] Elson, E.L. and Reidler, J.A. (1979) J. Supramol. Struct. 12, 481–489.
[20] Johansson, B., Sundqvist, T. and Magnusson, K.-E. (1987) Cell Biophys. 10, 233–244.
[21] Petersen, N.O., Höddelius, P.L., Wiseman, P.W., Seger, O. and Magnusson, K.-E. (1993) Biophys. J. 65, 1135–1146.
[22] Petersen, N.O. (1986) Biophys. J. 49, 809–815.
[23] Schlessinger, J. (1986) J. Cell Biol. 103, 2067–2072.
[24] Schreiber, A.B., Liberman, T.A., Lax, I., Yarden, Y. and Schlessinger, J. (1983) J. Biol. Chem. 258, 846–853.
[25] Van Belzen, N., Rijken, P.J., Hage, W.J., De Laat, S.W., Verkleij, A.J. and Boonstra, J. (1988) J. Cell. Physiol. 134, 413–420.
[26] Rönnstrand, L., Terracio, L., Claesson-Welsh, L., Heldin, C.-H. and Rubin, K. (1988) J. Biol. Chem. 263, 10429–10435.
[27] Carlsson, K. and Åslund, N. (1987) Appl. Opt. 26, 3232–3238.
[28] Heldin, C.-H., Ernlund, A., Rorsman, C. and Rönnstrand, L. (1989) J. Biol. Chem. 264, 8905–8912.
[29] Kusumi, A., Sako, Y. and Yamamoto, M. (1993) Biophys. J. 65, 2021–2040.